ACS Photonics

Article

pubs.acs.org/journal/apchd5

Statistical and Fourier Analysis for In-line Concentration Sensitivity in Single Molecule Dynamic-SERS

Thibault Brulé,[†] Alexandre Bouhelier, Hélène Yockell-Lelièvre,[†] Jean-Emmanuel Clément, Aymeric Leray, Alain Dereux, and Eric Finot*

Laboratoire Interdisciplinaire Carnot de Bourgogne, UMR 6303 CNRS, Université Bourgogne Franche-Comté, F-21078 Dijon, France

ABSTRACT: The Raman intensity fluctuations are the initial source of a lack of accuracy or reproducibility of SERS based nanosensors to reliably estimate the molecular concentration in microfluidics. Here, we show that the statistical analysis of the weighting of Raman scattering of the probed molecules compared to the photoluminescence of gold nanoparticles is particularly effective as a concentration indicator in a single molecule regime. We present a novel approach in the Fourier domain that is not limited by a multipoint precalibration or even the knowledge of the enhancement factor of the transducer. The analysis of pink noise in the frequency domain reveals a subdiffusion motion of individual adsorbed molecules in the hot-spot. The cutoff frequency between the white and pink noise is used to determine the in-line molecular concentration over a wide range between 10^{-11} and 10^{-6} M.

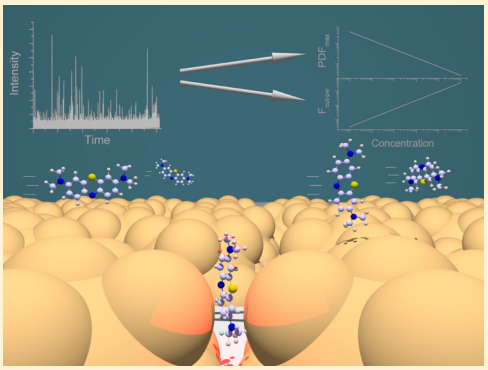

KEYWORDS: *Raman spectroscopy, nanosensor, methylene blue, photoluminescence, fractional Brownian noise, Freundlich isotherm, frequency domain, single molecule detection*

The medical diagnosis based on the early stage detection of biomarkers leads us to monitor traces of compounds in complex environments. Chemical nanosensors based on nanoparticles reach the ultimate detection limit[1] of a single molecule.[2] While extremely sensitive,[3] the fluorescent methods face the issue of selectivity:[4] sorting of molecules is limited by the number of fluorophores and the sample preparation thus excludes in-line measurement, i.e., a fast and dynamic measurement in real-time. Raman spectroscopy enhanced by the localized plasmonic resonance is of particular interest for sorting molecules if we consider its full potential of label free sensors and its selectivity provided by the ability to analyze the vibrational fingerprint of a single molecule.[5]

However, detecting the presence of a single molecule is not enough to quantify its in-line volume concentration in solution. The Raman events can thus be counted without being linearly correlated with changes in molecular concentration. Events related to concentrations as low as 10^{-18} M are observed by preconcentrating molecules on a large surface area over long integration time (8 h)[6] or by evaporating water. The intensity of Raman peaks increases then with the concentration. On the basis of this principle, a SERS immuno-sensor exhibits a wide linear range of mass concentration (0.1 pg/mL to 10 ng/mL) with a low limit of detection (LoD) of 7 fg/mL of human immunoglobulin G protein.[7] However, the integration of all events from a large surface prevents sorting different molecules using spectroscopy for single molecules. In addition, reliability of the quantification is hindered by poor uniformity of the SERS intensity leading to a poor reproducibility of the SERS signal, impeding the development of SERS based assays.[8] Plasmonic-based nanosensors,[10] in common with general sensors with sensitive areas on the scale of nanometers,[9] cannot be used directly to detect molecules dissolved in femto- or attomolar solutions. In other words, they are diffusion-limited, and their detection times are not practically feasible at such concentrations.[11] The combination of microfluidics and SERS based sensors is an advanced step forward, measuring in-line concentration.[12] The typical detection limit for a nanosensor such as rhodamine 6G is as low as 10^{-7} M with an average Raman enhancement factor EF[13] of 10^5. This detection limit for crystal violet is as low as 10^{-12} M for a Raman enhancement factor[14] as large as 10^7. The calibration of the nanosensors[15] depends then clearly on the enhancement factor, which can vary locally and from substrate to substrate[16] between 10^4 and 10^{15}.[17] The statistical distribution of the enhancement factor is governed by a Pareto law.[18] The objective is then to find a way to both guarantee the reliable selectivity in detecting a fingerprint of single events and to dose the molecules in-line in a reasonable time frame of 10 min.

Temporal fluctuations in SERS[19] have been already analyzed using the autocorrelation function[20] especially for monitoring the molecular diffusion, the dynamics of surface rearrangement,[21] and nanoparticles aggregation.[22] Here, we propose to examine the sensitivity of the nanosensor immobilized on the wall of microfluidics channels by analyzing the time series of the signal issued from a photon-counting system. Fluctuations will

Received: March 19, 2015
Published: August 11, 2015

DOI: 10.1021/acsphotonics.5b00134
ACS Photonics 2015, 2, 1266−1271

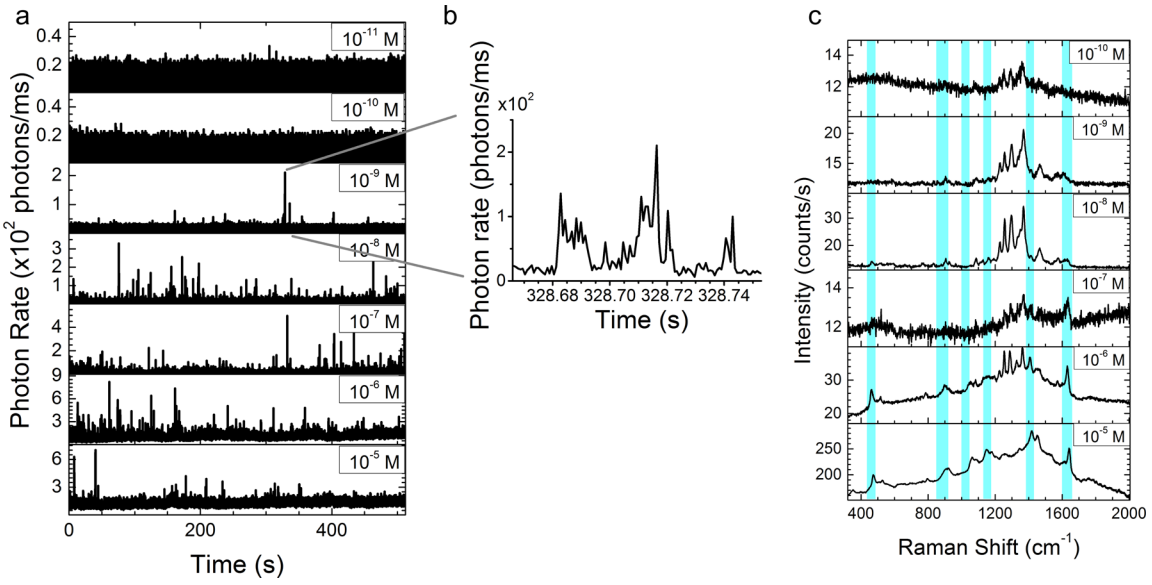

Figure 1. (a) Times series of the Raman counting rate as a function of the concentration in methylene blue. (b) Zoomed in image of Raman events at 10^{-9} M over a 80 ms time window. (c) SERS spectra of methylene blue. Each spectrum is related to a single event of its respective kinetics in panel a. Blue areas are identified Raman bands based on ref 25.

be first analyzed using the statistical intensity distribution, and we compare this to an innovative approach in SERS: the noise analysis in the frequency space using the Fourier transform. Molecular concentration can be deduced from both (i) the probability density function indicating the ratio between photoluminescence and Raman signals and (ii) the $1/f$ pink noise governed by the interaction of the Raman molecule with the surface enhanced electromagnetic field.

EXPERIMENTAL METHOD

Our SERS active substrate is based on a self-assembly of colloidal nanoparticles of 80 nm in diameter into prepatterned templates. Complex surface shaped raspberry-like gold nanoparticles (AuNPs) are immobilized on glass substrated capped with microfluidics channels as described previously in ref 23. AuNPs are then cleaned sequentially by oxidizing organics using an oxygen plasma cleaner and by rinsing off thoroughly using deionized water. Special care is taken to avoid surface contamination with substances such as colloid surfactants or the solution pollutants mainly arising from the release of the polymer constituents of the nonpassivated PDMS microfluidics. Methylene blue is used as a standard efficient Raman scatter. A specific experimental plan is designed to investigate the effect of both the EFs of the hot spot and the changes in concentration of methylene blue. The concentration ranged over 8 orders of magnitude between 10 pM and 10 μM. Spots easily retrievable on the SERS substrate using lithographed marks are statistically analyzed. A peristaltic pump is used to flow the solution at a flow rate of 2 μL/min through microfluidic channels.

Dynamic SERS measurements are conducted with use of a custom-built confocal Raman setup. The 785 nm laser light is focused on a diffraction-limited spot, using a water immersion high objective (60×, NA = 1.20). The area of the confocal excitation spot is estimated to be approximately 0.1 μm^2. The laser intensity is kept constant at 100 $\mu W \cdot cm^{-2}$. To discriminate the emitted Raman signal from other contributions, the signal is filtered through a dichroic mirror. Stokes photons scattered in the 250 to 2000 cm^{-1} spectral window are detected every 1 ms using an avalanche photodiode (APD). The magnitude of the signal is then expressed in terms of count rate (cts/s). Simultaneously to the APD detection, the SERS response is analyzed with a spectrometer associated with a cooled CCD camera cadenced at 1 s acquisition time. For each methylene blue concentration, 7 spots are separately probed during 512 s resulting in 512 spectra and 655,360 data points on the Avalanche PhotoDiode.

TIME DOMAIN ANALYSES

We first investigate the signal as the intensity of Raman events. Time series are shown in Figure 1A by varying the concentration of the MB over 7 concentration decades. Below a concentration of 10^{-10} M when the SERS substrate is cleaned and the microfluidics passivated by aging, no Raman event can be detected, which means that all Raman spectra are flat.

Measuring a concentration means being able to calibrate the hot spot and to determine sensitivity and the LoD. The LoD for our device is then 10^{-11} M of methylene blue, namely, around 3.19 pg/mL for 512 s of acquisition. This LoD can be considered as relatively high since the hot spot has the capability to detect a single molecule event. Indeed, the LoD is limited by the capture of the cross-section of the hot spot (the smaller the hot spot, higher is the LoD). In addition, since the AuNPs are on the wall of the microfluidics, the parabolic profile of the flow rate imposes a zero convection velocity of molecules at the surface. Thus, the molecules enter into the hot spot through a diffusion process. At 10^{-11} M, the average distance between molecules is estimated to 200 nm, i.e., it exceeds the plasmon penetration depth of the nanoparticles estimated around 100 nm, i.e., the particle size.[24] When increasing the concentration, between 10^{-10} and 10^{-6} M, the number of events and the intensity of the peaks increase concurrently. Figure 1B shows that the duration of highest peaks is 2−3 ms, whereas the lifetime of lower peaks increases up to tens of milliseconds. When exceeding 10^{-6} M, the signal baseline is no

DOI: 10.1021/acsphotonics.5b00134
ACS Photonics 2015, 2, 1266−1271

longer flat and slightly increases in amplitude, thereby reducing the peak height.

Counting the events as a function of concentration is not a suitable solution because correctly defining an event is nontrivial. Our initial analysis consists of evaluating the occurrence of Raman scattering by calculating the probability density function (PDF) of the photon rates (Figure 2) from the

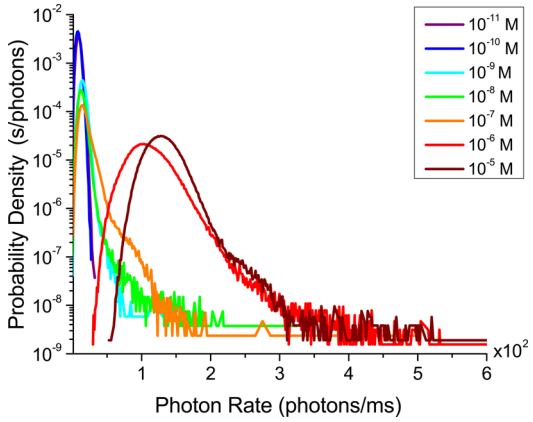

Figure 2. Probability density function of the Raman counting rate for each methylene blue concentration.

time series corresponding to Figure 1A. When focusing on AuNP in water, the photon rate fluctuates around 20 photons/ms. Indeed, we attribute this level of the gold photoluminescence (PL) that fluctuates with time due to an electron–hole recombination process.[26] The PL can serve as a retriever of the nanoparticles on the surface but also as an indicator of the surface state of the nanoparticles. Above 10^{-6} M, the mode of the distribution attributed to the PL shifts from 20 to 200 photons/ms and is broadened; this corresponds to the increasing and waving of the baseline in the time series (Figure 1A). We should attribute the increase in the PL to the oxidation of the AuNPs, namely, a chemisorption of the methylene blue on AuNPs responsible for charge transfer and also a continuous Raman contribution. This assertion is confirmed by comparing the spectra obtained between 10^{-10} and 10^{-5} M for single Raman events (Figure 1C). At lowest concentrations, the red shift of the 880, 1030, and 1390 cm^{-1} bands to, respectively, 920, 1062, and 1450 cm^{-1} are spectral proofs of chemisorption. The bands between 1200 and 1400 cm^{-1} are also characteristic as previously observed.[27] The more "standard" spectral fingerprint of methylene blue becomes more evident when increasing the concentration.

The Raman scattering corresponds to the right tail of the distribution in the continuity of PL distribution without a noticeable inflection point. Above a micromolar concentration, we switched from a single diffusive molecule regime to a more complex configuration involving multiple adsorbed molecules. The average distance between molecules in solution at 10^{-6} M is around 1 nm. The fact that the PL of AuNPs does not shift significantly at low concentration means that the EF of the spot remains stable throughout the measurement. With a laser of 0.1 mW power focused on an area (200 nm diameter), the incident laser photon flux is about $\Phi_0 \simeq 10^{16}$ photons/(10^{-13} m^2) = 10^{29} photons/m^2/s. Typically, the Raman photon rate I_s fluctuates between 50 and 500 photons/ms. By considering a 60% loss in microscope and APD collection (in the worst case), the enhancement factor can be obtained by $EF = I_s/(0.4\ \sigma\ \Phi_0)$, where σ is the accepted cross-section of our Raman reporter (10^{-26} to 10^{-28} cm^2). The resulting EF should be in the range of 10^4–10^7.

The statistical distribution of the intensity is used to investigate the partitioning between the PL (low intensity but continuous) and the Raman events (intense but rarer). Since the area under each curve of each PDF is normalized to 1, a broadening of the distribution due to the lengthening of the Raman tail would result in a decrease in the maximum probability density of the statistical intensity mode. This is calculated for 7 different spots at each concentration (e.g., for 10^{-9} M in Figure 3B).

The log–log plot of the PDF_{max} versus the photon rates in Figure 3B shows a straight line between 10^{-11} and 10^{-6}. This is characteristic of a relationship of power law $PDF_{max} = aC^k$ where a and k are the constant and power terms corresponding to the intercept and slope of the line, respectively. This power law can be modeled by a Freundlich isotherm,[28] which usually refers to heterogeneous molecular adsorption.[30] The Freund-

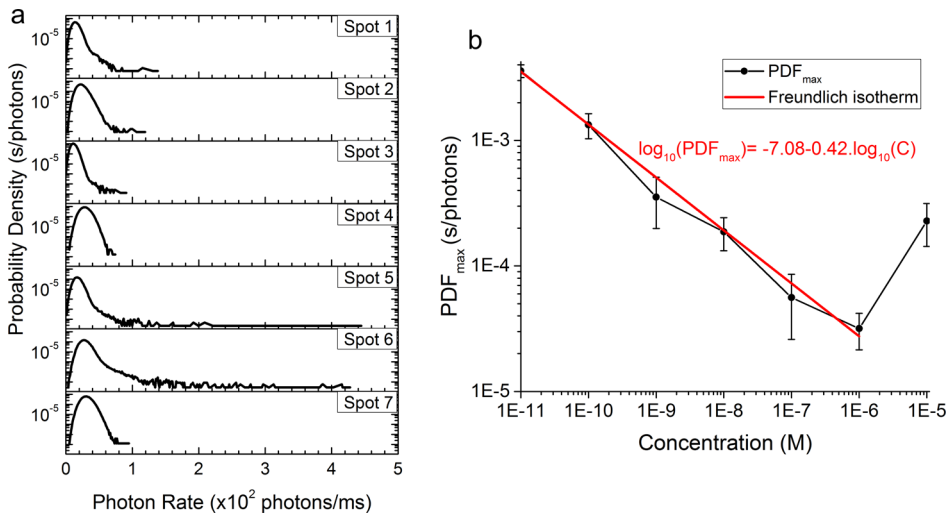

Figure 3. (a) Photon PDF distributions at 7 different spots at 10^{-9} M. (b) Evolution of PDF_{max} with methylene blue concentration. The error bars result of the analysis of the 7 different spots at each concentration.

DOI: 10.1021/acsphotonics.5b00134
ACS Photonics 2015, 2, 1266–1271

lich isotherm model applied here results in $\log_{10}(PDF_{max}) = \log_{10}(a) + k \log_{10}(C)$. We can thus define concentration sensitivity as follows: $k = \frac{\log_{10}(PDF_{max})}{\log_{10}(C)} = -0.42$.

Below 10^{-11} M, the probability density of PL is maximal. It confirms that the Raman signal is too sparse at such concentrations to be detected in 512 s. Above 10^{-6} M, the Raman signal becomes so important that the increase of the intensity baseline already reported in Figures 1 and 2 is composed by Raman and PL photons. Thus, the two phenomena cannot be easily distinguished at such concentrations.

The error bars in Figure 3B were calculated from the variance of the 7 spots spread on the sample. One can rely on the PDF_{max} as a reproducible parameter confirming the linear variation in the log−log plot of Figure 3B. One important point is that the definition of a the concentration sensitivity is then independent of the localization. Nevertheless, the shape and the length of the right tail attributed to the Raman contribution appears to vary strongly from one spot to another. It can therefore be concluded that the enhancement factor of the hot spot that also governs the PL should not vary significantly locally; the variability in intensity not locally reproducible should be then attributed to the orientation disorder of Raman molecules when placed into a well-defined polarized surface EM field. The heterogeneity of the vibrational fingerprints according to the molecular orientation toward the surface should explain the Freundlich isotherm model[28].

Although a concentration sensitivity was able to be defined using the probability density of the Raman events at each spot, the result is still system dependent, i.e., the objective focus, the laser power, and wavelength, but especially intensity dependent. The next approach is to get rid of the intensity dependence by analyzing the APD signal in the frequency domain using a simple Fourier transform.

FREQUENCY DOMAIN APPROACH

The fast Fourier transform (FFT) is a mathematical operation to represent frequency (on an exponential basis) signals that are not necessary periodic. Transforming the temporal dynamics of Raman events to its frequency spectrum allows one in particular to highlight the decay of the power spectral density (PSD) with frequency in order to sort the sources of noise.

Applied to the time series at each concentration (Figure 4), the FFT was used to identify two key sources of noise.

A constant *PSD* over the frequency *f* is typical of white noise, namely, a stochastic process corresponding to zero autocorrelation (or total independence). On Figure 4, this white noise is easily recognizable by the plateau (0 dB/Hz slope). This decorrelation in the frequency domain is quite consistent with a statistical distribution of the normal law "Gaussian" mean and variance data observed for the PL where almost no Raman events related to methylene blue was detected. When the PL increases as observed on the *PDF* plot at high concentrations (>10^{-6} M), a higher *PSD* of the white noise is also observable in the frequency domain. The plateau at 13 dB typically corresponds to the PL photon rate: 10 $\log_{10}(20)$.

Increasing the concentration shows a reduction of the white noise range in favor of a low frequency dependence of the *PSD*. Pink noise or $1/f$ noise corresponds in the log−log graph of Figure 4 to a decrease in *PSD* by −10 dB per frequency decade. The *PSD* can be then fitted by the law $PSD_{pink} = -10\ log_{10}(f) + PSD_o$. This pink noise is characteristic of the appearance of the bright Raman events in the time series. In fact, the bright events can be as short as 1 ms, and the average time between bright peaks can reach 10 s. To understand this phenomenon's origins, it is necessary to consider the diffusive motion of the molecules. The average distance d between molecules varies with the changes in concentration. d can be approximated by considering that the volume occupied by a single molecule $4\pi d^3/3 = 1/N_A C$ with N_A being the Avogadro number. Typically, when changing C from 10^{-11} M to 10^{-6} M, d decreases to tens of micrometers to a few nanometers. If the mean free path length d is less than the boundary layer thickness in microfluidics, the molecules will therefore not reach the cross-section of the nanosensor. d is thus concentration dependent. The diffusion speed of a molecule is given by $V_d = 3D/d$, where D is the diffusion coefficient equal to 10^{-10} m^2/s. V_d varies between 20 μm/s (high C) and 10 mm/s (low C). Considering a sensor cross-section of 100 nm field, the residence time of the molecule in the area of interaction with the nanosensor is between milliseconds (high C) to 10 μs (low C), and this time is then faster than what is measured in our experiment. The diffusion process is Poissonian, which implies that the variance is equal to the number of events. A normal distribution of molecules in the spot cannot explain the signal variations and the long residence time observed. So, the lifetime of Raman events are related to the adsorption of molecules onto the surface of the nanoparticles. It is observed that this residence time τ does not depend on the concentration. It is determined by the formula of Frenkel: $\tau = \tau_o \exp(E/k_bT)$ where $\tau_o = 10^{-13}$ s, where T the temperature, and E is the energy between the molecule and the substrate.[29] Typically, physisorption (E = 10−100 meV) and chemisorption (E = 1−10 eV) are not measured, and in our case, we are facing a quasi chemisorption (E = 0.6−0.7 eV) such as hydrogen bonding which induces time commensurable from 1 to 100 ms.

We define f_{pw} as the cutoff frequency between the pink noise and the white noise, typically the intercept between the line PSD_{pink} and the value 13 dB. The log−log plot of f_{pw} versus the concentration (Figure 5) shows a Freundlich isotherm as already observed in the statistical analysis; in this case, $f_{pw} = f_o C^h$, where h = 0.61. h is an heterogeneity parameter indicative of the strength of the adsorption; the smaller the h, the greater the expected heterogeneity. The heterogeneity can be thought of here spectrally as a collection of vibration features. A value of

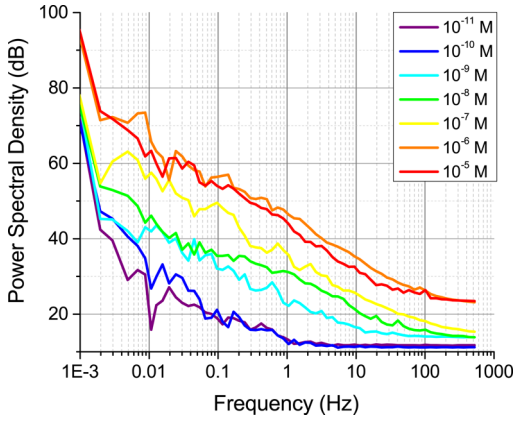

Figure 4. Point spread density characteristics of the photon counting versus frequencies at each concentration.

DOI: 10.1021/acsphotonics.5b00134
ACS Photonics 2015, 2, 1266−1271

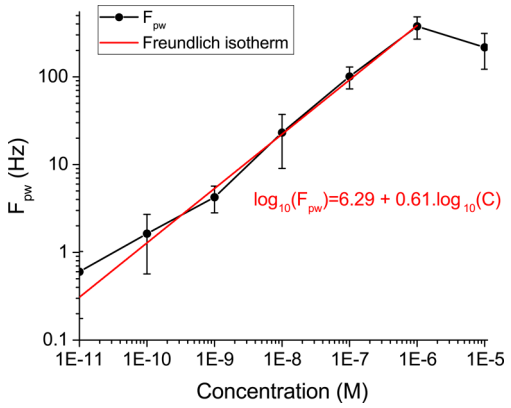

Figure 5. Evolution of the cutoff frequency f_{pw} between pink and white noises with the methylene blue concentration. The errors bar result of the analysis of 7 different spots for each concentration.

h lying between 0.1 and 1 indicates a favorable chemisorption process.[30] The saturation of f_{pw} at high concentration is mostly explained by the sampling rate of the APD at 3 ms (300 Hz); the upper value of the detection limit in concentration is then limited to sampling time of the APD. Since at very low concentration f_{pw} deviates from the Freundlich trend, the LoD can then be placed at 10^{-11} M. By considering f_{pw} as the minimum number of detected molecules per second, the single molecule regime is clearly reached with separated time span between molecules of 1 s, which is a reasonable time necessary to disperse the Raman photon spectrally on a spectroscope. The determination of concentration using the counting of single molecules seems more accurate at low concentration. This fact may be explained by the fact that at high concentration we progressively quit the regime of single molecules where molecules can be separated. At high concentrations, the diffusion time of molecules increases to millisecond range and overlaps the adsorption time.

The error bars shown in Figure 5 are based on the analysis of 7 different spots, each one giving a comparable response. So the ergodicity of the analysis is demonstrated even at the single molecular level and is of high interest thinking about the development of an in-line sensor that implies using a reliable method without precalibration.

The main interests of this approach remain in the determination of sensitivity: $\log_{10}(f_{pw})/\log_{10}(C)$ equals to h, which should be "universal" as the force strength between the Raman molecule and the surface of the hot spot. The fact that h is independent of the hot spot localization over the sample demonstrates the high spatial repeatability and the ergodicity of the approach.

DISCUSSION

In this study, we show that statistical analysis in intensity is complementary to the Fourier analysis for determining the molecular concentration. Our approach has allowed the resolution of the problem of the high spatial variability of the Raman intensity in the single molecule regime.

Thus, molecular concentration can be deduced from (i) the probability density of the mode of the photon rate distribution. It corresponds to the weight factor between the Raman scattering and the gold photoluminescence. (ii) The cutoff frequency between the $1/f$ pink noise and the white noise in the Fourier transform of the time series of photon scattering. The concentration dependent temporal fluctuation of a nanosensor takes its origin in the pink noise explained by the subdiffusive process of Raman scattering in the hot spot, namely, the lack of a characteristic time scale in the waiting times (off time). The observed intermittent Raman events correspond to the chemical adsorption of molecules on gold. Time varying from 1 to 100 ms is commensurable to a quasi chemisorption.

Both approaches enable establishing an excellent logarithmic sensitivity over 5 decades of concentration of methylene blue simply governed by a Freundlich isotherm model. However, the error in determining the concentration depends on the methods. The less precise one is based on intensity fluctuations. We have shown that EF of one hot spot remains unchanged with time during the measurement. This is explained by the stability of GNPs immobilized on the surface. However, the geometry of the hot spot can strongly vary from one spot to another as shown in Figure 3a. The intensity of the brightest events cannot be used to calibrate the sensor. Statistics based on the probability density function have greatly reduced the error bar (Figure 3b), but still the error bars around one decade of concentration can be determined accurately over 6 orders of magnitude. The most accurate method is based on the temporal fluctuations (Fourier analysis) which was found independent of the variability of the hot spot. Figure 5a shows that the concentration can be determined more precisely with an accuracy of 10% for one decade. The calibration of the sensor is not required in this method. For both methods, we have shown that the main sources of error are due to the preparation of the SERS active sensors, in particular the cleanness of the nanoparticle which was cleaned using a plasma cleaner. We intend in this work, to demonstrate that the Fourier analysis marks a first step in tackling the calibration issue. Seven locations on the samples have shown that the Fourier transform of the kinetics of adsorption of molecules is a powerful and robust analysis: the incomplete knowledge of the enhancement factor does not restrict the kinetics of molecular counting. The number of molecules adsorbed appears to be more reproducible from one spot to another compared to the Raman intensity, which depends on the position of the molecule within the field gradient.

AUTHOR INFORMATION

Corresponding Author

*E-mail: eric.finot@u-bourgogne.fr.

Present Address

†(T.B. and H.Y.-L.) Département de Chimie, Université de Montréal, CP 6128 Succ. Centre-Ville, Montréal, QC, Canada H3C 3J7.

Notes

The authors declare no competing financial interest.

ACKNOWLEDGMENTS

This work was supported by the European project SPEDOC (FP7-ICT-2009-4) under Grant agreement No. 248835 in cooperation with the Labex ACTION program (contract ANR-11-LABX-01-01). This work was performed in the context of the European COST action MP1302 Nanospectroscopy.

REFERENCES

(1) Kneipp, K.; Wang, Y.; Kneipp, H.; Perelman, L. T.; Itzkan, I.; Dasari, R.; Feld, M. S. Single molecule detection using surface-

DOI: 10.1021/acsphotonics.5b00134
ACS Photonics 2015, 2, 1266−1271

enhanced Raman scattering (SERS). *Phys. Rev. Lett.* **1997**, *78*, 1667−1670.
(2) Nie, S. M.; Emery, S. R. Probing single molecules and single nanoparticles by surface-enhanced Raman scattering. *Science* **1997**, *275*, 1102−1106.
(3) Qian, Z. S.; Shan, X. Y.; Chai, L. J.; Ma, J. J.; Chen, J. R.; Feng, H. DNA nanosensor based on biocompatible graphene quantum dots and carbon nanotubes. *Biosens. Bioelectron.* **2014**, *60*, 64−70.
(4) Su, S.; Fan, J.; Xue, B.; Yuwen, L.; Liu, X.; Pan, D.; Wang, L. DNA-conjugated quantum dot nanoprobe for high-sensitivity fluorescent detection of DNA and micro-RNA. *ACS Appl. Mater. Interfaces* **2014**, *6*, 1152−1157.
(5) Pieczonka, N. P. W.; Aroca, R. F. Single molecule analysis by surfaced-enhanced Raman scattering. *Chem. Soc. Rev.* **2008**, *37*, 946−54.
(6) Etchegoin, P.; Maher, R. C.; Cohen, L. F.; Hartigan, H.; Brown, R. J. C.; Milton, M. J. T.; Gallop, J. C. New limits in ultrasensitive trace detection by surface enhanced Raman scattering (SERS). *Chem. Phys. Lett.* **2003**, *375*, 84−90.
(7) Li, M.; Cushing, S. K.; Zhang, J.; Suri, S.; Evans, R.; Petros, W. P.; Wu, N. Three-dimensional hierarchical plasmonic nano-architecture enhanced surface-enhanced Raman scattering immunosensor for cancer biomarker detection in blood plasma. *ACS Nano* **2013**, *7*, 4967−4976.
(8) Lim, D. K.; Jeon, K. S.; Hwang, J. H.; Kim, H.; Kwon, S.; Suh, Y. D.; Nam, J. M. Highly uniform and reproducible surface-enhanced Raman scattering from DNA-tailorable nanoparticles with 1-nm interior gap. *Nat. Nanotechnol.* **2011**, *6*, 452−460.
(9) Jing, C.; Shi, L.; Liu, X.; Long, Y. T. A single gold nanorod as a plasmon resonance energy transfer based nanosensor for high-sensitivity Cu(ii) detection. *Analyst* **2014**, *139*, 6435−6439.
(10) Witlicki, E. H.; Andersen, S. S.; Hansen, S. W.; Jeppesen, J. O.; Wong, E. W.; Jensen, L.; Park, U. V. Turning on Resonant SERRS Using the Chromophore - Plasmon Coupling Created by Host - Guest Complexation at a Plasmonic Nanoarray. *J. Am. Chem. Soc.* **2010**, *132*, 6099−6107.
(11) De Angelis, F.; Gentile, F.; Mecarini, F.; Das, G.; Moretti, M.; Candeloro, P.; Di Fabrizio, E. Breaking the diffusion limit with super-hydrophobic delivery of molecules to plasmonic nanofocusing SERS structures. *Nat. Photonics* **2011**, *5*, 682−687.
(12) Connatser, R. M.; Cochran, M.; Harrison, R. J.; Sepaniak, M. J. Analytical optimization of nanocomposite surface-enhanced Raman spectroscopy/scattering detection in microfluidic separation devices. *Electrophoresis* **2008**, *29*, 1441−1450.
(13) Fang, H.; Zhang, C. X.; Liu, L.; Zhao, Y. M.; Xu, H. J. Recyclable three-dimensional Ag nanoparticle-decorated TiO2 nanorod arrays for surface-enhanced Raman scattering. *Biosens. Bioelectron.* **2015**, *64*, 434−441.
(14) Zhang, C. X.; Liu, L.; Jun Yin, H.; Fang, H.; Mei Zhao, Y.; Jian Bi, C.; Jun Xu, H. Recyclable surface-enhanced Raman scattering template based on nanoporous gold film/Si nanowire arrays. *Appl. Phys. Lett.* **2014**, *105*, 011905.
(15) Hu, P.; Zhou, X.; Wu, Q. A new nanosensor composed of laminated samarium borate and immobilized laccase for phenol determination. *Nanoscale Res. Lett.* **2014**, *9*, 76.
(16) Hering, K.; Cialla, D.; Ackermann, K.; Dörfer, T.; Möller, R.; Schneidewind, H.; Popp, J. SERS: a versatile tool in chemical and biochemical diagnostics. *Anal. Bioanal. Chem.* **2008**, *390*, 113−124.
(17) Li, M.; Cushing, S. K.; Zhang, J.; Lankford, J.; Aguilar, Z. P.; Ma, D.; Wu, N. Shape-dependent surface-enhanced Raman scattering in gold-Raman probe-silica sandwiched nanoparticles for biocompatible applications. *Nanotechnology* **2012**, *23*, 115501.
(18) Fang, Y.; Seong, N. H.; Dlott, D. D. Measurement of the Distribution of Site Enhancements in Surface-Enhanced Raman Scattering. *Science* **2008**, *321*, 388−393.
(19) Weiss, A.; Haran, G. Time-Dependent Single-Molecule Raman Scattering as a Probe of Surface Dynamics. *J. Phys. Chem. B* **2001**, *105*, 12348−12354.
(20) Barbara, A.; Dubois, F.; Ibanez, A.; Eng, L. M.; Quemerais, P. SERS Correlation Spectroscopy of Silver Aggregates in Colloidal Suspension: Quantitative Sizing Down to a Single Nanoparticle. *J. Phys. Chem. C* **2014**, *118*, 17922−17931.
(21) Laurence, T. A.; Braun, G. B.; Reich, N. O.; Moskovits, M. Robust SERS enhancement factor statistics using rotational correlation spectroscopy. *Nano Lett.* **2012**, *12*, 2912−2917.
(22) Schrof, W.; Klingler, J.; Rozouvan, S.; Horn, D. Raman correlation spectroscopy: A method for studying chemical composition and dynamics of disperse systems. *Phys. Rev. E: Stat. Phys., Plasmas, Fluids, Relat. Interdiscip. Top.* **1998**, *57*, R2523−R2526.
(23) Brule, T.; Yockell-Lelievre, H.; Bouhelier, A.; Margueritat, J.; Markey, L.; Leray, A.; Finot, E. Sorting of Enhanced Reference Raman Spectra of a Single Amino Acid Molecule. *J. Phys. Chem. C* **2014**, *118*, 17975−17982.
(24) Read, T.; Olkhov, R. V.; Shaw, A. M. Measurement of the localised plasmon penetration depth for gold nanoparticles using a non-invasive bio-stacking method. *Phys. Chem. Chem. Phys.* **2013**, *15*, 6122−6127.
(25) Naujok, R. R.; Duevel, R. V.; Corn, R. M. Fluorescence and Fourier Transform Surface-Enhanced Raman Scattering Measurements of Methylene Blue Adsorbed onto a Sulfur-Modified Gold Electrode. *Langmuir* **1993**, *9*, 1771−1774.
(26) Yuan, C. T.; Chou, W. C.; Tang, J.; Lin, C. A.; Chang, W. H.; Shen, J. L.; Chuu, D. S. Single fluorescent gold nanoclusters. *Opt. Express* **2009**, *17*, 16111−16118.
(27) Tognalli, N. G.; Fainstein, A.; Vericat, C.; Vela, M. E.; Salvarezza, R. C. Exploring three-dimensional nanosystems with Raman spectroscopy: methylene blue adsorbed on thiol and sulfur monolayers on gold. *J. Phys. Chem. B* **2006**, *110*, 354−360.
(28) Yang, C. Statistical Mechanical Study on the Freundlich Isotherm Equation. *J. Colloid Interface Sci.* **1998**, *208*, 379−387.
(29) Kreuzer, H. J. Desorption Kinetics. *Faraday Discuss. Chem. Soc.* **1985**, *80*, 265−276.
(30) Jaroniec, M. Adsorption on heterogeneous surfaces: the exponential equation for the overall adsorption isotherm. *Surf. Sci.* **1975**, *50*, 553−564.

DOI: 10.1021/acsphotonics.5b00134
ACS Photonics 2015, 2, 1266−1271